



# Fabricating a bulk FCC Hf by a combination of high-energy ball milling and spark plasma sintering

Kun Luo, Song Ni\*, Min Song\*

State Key Laboratory of Powder Metallurgy, Central South University, Changsha 410083, China

## ARTICLE INFO

### Keywords:

Hafnium  
High-energy ball milling  
SPS  
Phase transformation

## ABSTRACT

A face-centered-cubic (FCC) hafnium (Hf) in bulk was fabricated by a combination of high-energy ball milling and spark plasma sintering (SPS). The hexagonal-close-packed (HCP) Hf powder as the raw material was transformed into FCC phase during ball milling, and the HCP to FCC transformation also occurred when applying SPS on the ball milled powder. The effects of grain size, impurities and structural instability introduced during high-energy ball milling process on the HCP to FCC phase transformation were discussed. In addition, due to the grain boundary strengthening and second phase strengthening, the hardness of the bulk FCC Hf was greatly increased to above 1200 Hv.

## 1. Introduction

Hafnium (Hf) possesses high melting point, high density and strength, large cross-section for thermal neutron capture, and excellent corrosion resistance [1–4]. Because of these superior properties, it has been used as control rods in nuclear reactors, filaments and electrodes in electronic devices and solid solution strengthening element in many superalloys [5–7]. Hf exhibits various crystal structures under different conditions. Under equilibrium condition, it is of a hexagonal-close-packed (HCP) crystal structure at room temperature, and a body-centred cubic (BCC) crystal structure at temperature above 2016 K. The HCP phase can transform to a simple hexagonal crystal structure under a pressure of 22–38 GPa [8–10]. Interestingly, a face-centered-cubic (FCC) Hf, which is not present in the equilibrium phase diagram of Hf, has been reported in recent years. The FCC Hf can be obtained by high energy ball-milling Hf powder with HCP structure [1,11] or cold-rolling bulk HCP Hf [12]. Similar allotropic change has also been reported in other IVB group elements such as Ti [13,14], Zr [15,16] and some other metals such as Co [17], Fe [18] and Nb [19]. Several mechanisms were proposed for the HCP to FCC phase transformation. Manna et al. [13] proposed that structural instability caused by plastic strain, increasing lattice expansion and negative hydrostatic pressure introduced during high-energy ball milling is responsible for the HCP to FCC phase transformation in the ball milled powders. Seelam et al. [20] pointed out that impurities introduced during ball milling are necessary for the phase transformation. Xiong et al. [21] proposed that the FCC phase Hf is a small-size stable phase and the HCP to FCC phase transformation can occur when the grain size decreases to a critical value ( $< 10$  nm).

Such small grain size can be realized during high-energy ball milling. However, Zhao et al. [12,16] reported the HCP to FCC phase transformation in cold-rolled bulk Hf [12] and Zr [16] recently with grain sizes ranging from several micro-meters to several hundred nanometers. They proposed that the phase transformation was achieved via partial dislocation emission from every second basal plane or via pure-shuffle and shear-shuffle mechanisms [12,16]. Therefore, no consensus has been reached for the formation mechanism and the factors affecting the stability of the FCC phase. From our previous research, pure FCC phase Hf can be obtained by high-energy ball milling the HCP Hf powder to  $> 10$  h, but it is difficult to achieve complete FCC Hf in bulk by applying large strain on bulk HCP Hf. It's worth mentioning that pure FCC Hf in bulk has never been fabricated before and the mechanical properties of the bulk FCC Hf have never been investigated. Therefore we propose to fabricate the pure FCC Hf in bulk through a combination of ball milling and spark plasma sintering (SPS) processes.

SPS is an advanced technique to synthesize bulk material, which is increasingly popular in recent years due to the excellent performance in comparison to the traditional solidification method such as hot pressing [22] and isostatic pressing [23]. The heating rate of an SPS process can be up to 1000 °C per minute [24–26], which can boost the solidification process. The as-sintered samples usually exhibit fine grain size and superior performance [27,28].

In this study, a complete FCC Hf in bulk was fabricated by a combination of high-energy ball-milling and SPS. X-ray diffraction (XRD), scanning electron microscopy (SEM) and transmission electron microscopy (TEM) were applied to investigate the microstructures of the raw powder, as-milled powders and as-sintered bulk samples.

\* Corresponding authors.

E-mail addresses: [song.ni@csu.edu.cn](mailto:song.ni@csu.edu.cn) (S. Ni), [msong@csu.edu.cn](mailto:msong@csu.edu.cn) (M. Song).

Microhardness tests were carried out on the as-sintered samples. The effects of grain size, impurities and structural instability introduced during high-energy ball milling on the HCP to FCC phase transformation were discussed.

## 2. Experimental

Hf powder (> 99 wt%) of 400 mesh (~37  $\mu\text{m}$  particle size) was high-energy ball milled in stainless tanks by a planetary ball miller. The volume of per stainless tank is ~402  $\text{cm}^3$ . 30 g powder was mixed with 300 g stainless balls in each tank. The weight ratio of ball to powder is 10:1. 0.3 g stearic acid was added as control agent to prevent cold welding and minimize agglomeration of the powder particles and adherence to the balls and the tank. The powder was milled at a speed of 300 rpm for 10 h and 20 h in single direction and bi-direction modes. In single direction mode, the powder was milled for 25 min and paused for 5 min, then was milled for another 25 min in the same direction and paused for another 5 min. In bi-direction mode, the powder was milled clockwise for 25 min and paused for 5 min, then was milled anti-clockwise for 25 min and paused for 5 min. The milling process was continued until 10 h or 20 h was reached. It's worth mentioning that in single direction mode, the powder is easier to adhere to the inner wall of the milling tank compared with that in bi-direction mode. Therefore, as the milling time increased, the ratio of ball to powder in single direction mode will be a little higher than that in bi-direction mode. An argon glove-box was used for sampling to avoid oxidation and nitridation. The parameters for ball-milling were shown in Table 1.

The as-milled powders with different milling time and different rotation modes were spark plasma sintered on an FCT HP D 25/3 (FCT, Germany) spark plasma sintering furnace under a vacuum condition (< 0.5 mbar). The sintering temperature was measured using a thermocouple inserted in the die through a drilled hole. In the sintering process, powders were insulated with graphite die by graphite foils to protect the mould. The powder was heated to 800  $^{\circ}\text{C}$  and held for 8 min, then cooled down to the room temperature. The heating rate was 100  $^{\circ}\text{C}$  per min. A uniaxial pressure of 80 MPa was applied during the sintering process. The as-sintered sample was polished using SiC abrasive paper to remove the carbon impact layer.

The phase compositions, crystal structures of the raw powder, as-milled powder and as-sintered bulk samples were characterized by XRD, SEM and TEM. The XRD measurements were carried out on a Dmax 2500VB diffractometer in Bragg-Brentano geometry, using Cu-K $\alpha$  radiation ( $\lambda = 0.1542 \text{ nm}$ ). The diffraction data were acquired over the scattering angle from 20 $^{\circ}$  to 80 $^{\circ}$  with a step size of 0.02 $^{\circ}$  and acquisition time of 4 $^{\circ}$  per min. The SEM observations were carried out on an Helios Nanolab G3 UC scanning electron microscope using an in-column Everhart Thornley detector. The TEM observations were carried out on an FEI Tecnai G20 TEM operating at 200 kV. For the powder samples, a small amount of powder was put into a beaker and mixed with ethanol. The solution was ultrasonically dispersed for 20 min and then a little suspension was dropped to a carbon film for TEM observation. For the bulk samples, a foil with the thickness of 0.1 mm was cut from the as-sintered sample in perpendicular to the compression direction. Then it was grounded to 50  $\mu\text{m}$  and ultimately polished by Ar $^{+}$  ion-thinning (Gatan 691 PIP). Micro-hardness test with a load of 20 kg and holding time of 10 s was applied to assess the mechanical property of the as-

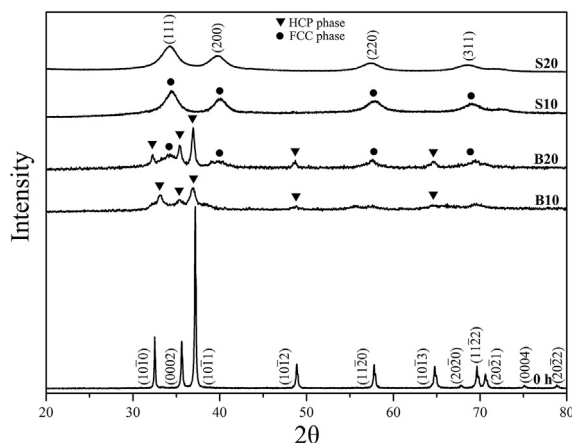


Fig. 1. XRD patterns of the powder before ball milling and after ball milling with different modes and various time.

sintered samples.

## 3. Results and discussion

### 3.1. Ball milling process

Fig. 1 shows the XRD patterns of the raw powder and the milled powders with different milling rotation modes and time. The raw powder exhibits a single HCP phase. After high-energy ball milling, some new peaks as indicated by black dots appeared. The positions of the new peaks are 34.9 $^{\circ}$ , 40.1 $^{\circ}$ , 58.7 $^{\circ}$  and 69.8 $^{\circ}$ , which can be indexed to lattice planes of {111}, {200}, {220} and {311} of an FCC Hf. Comparing the XRD patterns of B10 and S10 samples, the FCC peaks were only shown in S10 sample but not shown in B10 sample, indicating that the HCP to FCC phase transformation is much faster under the single direction rotation mode. As the milling time increased to > 10 h, the ratio of ball to powder in single direction mode is higher than that in bi-direction mode, resulting in a higher milling efficiency and promoting the phase transformation. Continued milling the B10 sample to 20 h, the intensities of HCP peaks decreased and the peaks of FCC Hf appeared. Comparing the XRD patterns of S20 and S10 samples, the positions of the peaks are the same while the peaks of the S20 sample are more broadening than that of the S10 sample, indicating a finer grain size and/or higher lattice strain in the S20 sample after high-energy ball milling. The grain size can be calculated according to the Scherrer equation [29]:

$$t = \frac{0.9\lambda}{B \cos \theta} \quad (1)$$

where  $t$  is the average grain size,  $\lambda$  is the wavelength of the X-ray,  $B$  is the full width of half maximum intensity, and  $\theta$  is the Bragg diffraction angle. For the S10 powder, the grain size is calculated to be ~6.5 nm and for the S20 sample the grain size decreased to ~4.2 nm. For the B20 powder, the average crystallite size of the HCP phase is ~10.4 nm and for FCC phase the average grain size is ~5.5 nm. From the above calculated results, the average grain size of FCC phase is smaller than that of the HCP phase. It is important to realize that the Scherrer equation provides a lower bound on the particle size due to the reason that besides crystallite size, inhomogeneous strain and crystal lattice imperfections can also contribute to the width of a diffraction peak. The calculated results were also compared with the statistics of TEM observations. Though the exact grain sizes estimated from the two methods are different, the grain sizes exhibit the same variation tendency for different samples and different phases.

Fig. 2 shows high-resolution TEM images and the corresponding selected area electron diffraction (SAED) patterns of the S10 and B20

Table 1  
Parameters for high-energy ball milling.

Sample	Milling Mode	Milling Time(h)
S10	Single-direction	10
S20	Single-direction	20
B10	Bi-direction	10
B20	Bi-direction	20

Download English Version:

<https://daneshyari.com/en/article/7989544>

Download Persian Version:

<https://daneshyari.com/article/7989544>

[Daneshyari.com](https://daneshyari.com)